IL NUOVO CIMENTO Vol. 35 C, N. 6 Novembre-Dicembre 2012
DOI 10.1393/ncc/i2012-11353-y

Colloquia: LaThuile12

First results on Θ_{13} from the Double Chooz reactor antineutrino experiment

B. Reinhold(*) for the Double Chooz Collaboration
MPIK Heidelberg - Saupfercheckweg 1, D-69117 Heidelberg, Germany

ricevuto il 7 Settembre 2012

Summary. — Double Chooz is an electron antineutrino disappearance experiment observing neutrinos originating from the Chooz nuclear power plant and interacting in our detector. The flux of electron anti-neutrinos is altered through neutrino oscillations and thereby allows to measure Θ_{13}. The Double Chooz Collaboration published first results on its search for the neutrino mixing angle Θ_{13} in 2011. The current analysis comprises about 100 days of data taken since April 2011. Performing a so-called rate+shape analysis, a best-fit value for $\sin^2 2\Theta_{13} = 0.086$ is reported with uncertainties of ± 0.041 (stat) ± 0.030 (syst) using $\Delta m^2_{13} = 2.4 \cdot 10^{-3}\,\mathrm{eV}^2$. This article provides details about the analysis that lead to this result.

PACS 14.60.Pq – Neutrino mass and mixing.
PACS 13.15.+g – Neutrino interactions.
PACS 25.30.Pt – Neutrino-induced reactions.
PACS 95.55.Vj – Neutrino, muon, pion, and other elementary particle detectors; cosmic ray detectors.

1. – Introduction

Neutrino oscillations are by now a well-established model to explain experimental data from a wide variety of experiments. Be it solar- or atmospheric-neutrino experiments or experiments observing man made neutrinos from dedicated beams or reactors. Neutrino oscillations originate from the fact that neutrino flavour eigenstates are different from mass eigenstates. The flavour eigenstates are related to the mass eigenstates through the so-called PMNS([1]) mixing matrix which can be parameterized by three mixing angles Θ_{12}, Θ_{23}, Θ_{13} and a CP-violating phase δ. Additionally, neutrino oscillations require non-zero differences of neutrino masses squared: Δm^2_{13} and Δm^2_{23}. Two of the three mixing angles are found to be large or even close to maximal whereas until recently

(*) E-mail: Bernd.Reinhold@mpi-hd.mpg.de
([1]) PMNS: Pontecorvo, Maki, Nakagata, Sakawa.

© Società Italiana di Fisica

only upper limits existed for the third mixing angle Θ_{13}. δ-CP is hardly constrained by experimental data. This was still the situation at the beginning of 2011. Then indications for a finite Θ_{13} were reported by both the MINOS and T2K experiments in the $\nu_\mu \to \nu_e$ appearance channel [1, 2].

End of 2011 Double Chooz was the first of a second generation of reactor antineutrino experiments to report its results in the search of Θ_{13} [3]. In early 2012 both the Daya Bay and RENO reactor antineutrino experiments found similar best fit results for $\sin^2 2\Theta_{13}$ with higher significance [4,5]. A finite Θ_{13} opens the possibility to measure CP violation in the neutrino sector and the mass hierarchy in the near future.

2. – Oscillation probability

The survival probability $\mathcal{P}_{\overline{\nu}_e \to \overline{\nu}_e}$ for electron antineutrino is

$$\mathcal{P}_{\overline{\nu}_e \to \overline{\nu}_e}(L, E) = 1 - \sin^2(2\Theta_{13}) \sin^2 \left(1.27 \Delta m^2_{13}[eV^2] \frac{L[m]}{E[MeV]} \right), \tag{1}$$

in the approximation of small $\frac{L}{E}$, with L being the distance between reactor and detector and E is the energy of the antineutrino $\overline{\nu}_e$. As the neutrino energy spectrum coming from the reactor is known to have its maximum at around 3 MeV and $\Delta m^2_{13} = 2.4 \cdot 10^{-3}\,\mathrm{eV}^2$, one can calculate from formula (1) that a detector, located at 1.05 km from the two reactor cores is close to the oscillation maximum and is thereby sensitive to Θ_{13}.

3. – The Double Chooz detector

3˙1. *Two-detectors concept.* – The current generation of reactor neutrino experiments all adopt a two or multi detector concept in order to reduce systematic uncertainties. In case of Double Chooz the Near Detector will be placed at 410 m distance from the two reactor cores and the Far Detector is located at 1.05 km from the antineutrino source.

While the neutrino flux and spectrum at the Far Detector is altered through neutrino oscillations, namely by Δm^2_{13} and Θ_{13}, the Near Detector observes an almost unoscillated spectrum regardless of the actual value of Θ_{13} and so the ratio of the Far and Near Detector spectrum allow to extract Θ_{13}. Systematic uncertainties in the antineutrino flux coming from the reactors cancel. Absolute systematic uncertainties in the estimation of backgrounds, efficiencies or in the detector response reduce, so that only relative uncertainties remain. These relative uncertainties are substantially smaller than the absolute uncertainties.

Since the Near Detector is still under construction, for the current analysis only data of the Far Detector has been used and the analysis has been performed by comparing a measured neutrino spectrum to a predicted spectrum, which was calculated from reactor data and propagated through a detailed Monte Carlo (MC) simulation of the detector. The Monte Carlo simulation of the detector is based on GEANT4 [6] and has been tuned using calibration data. Many of the systematic uncertainties are estimated from remaining discrepancies between data and MC simulations.

3˙2. *Detection principle.* – The electron anti-neutrinos are detected via the Inverse Beta Decay (IBD) interaction on proton: $\bar{\nu_e} + p \to n + e^+$ ($E_{threshold} = 1.8\,\mathrm{MeV}$). The positron, which receives basically all the kinetic energy of the neutrino (minus the threshold energy), deposits its energy in the scintillator and eventually annihilates with

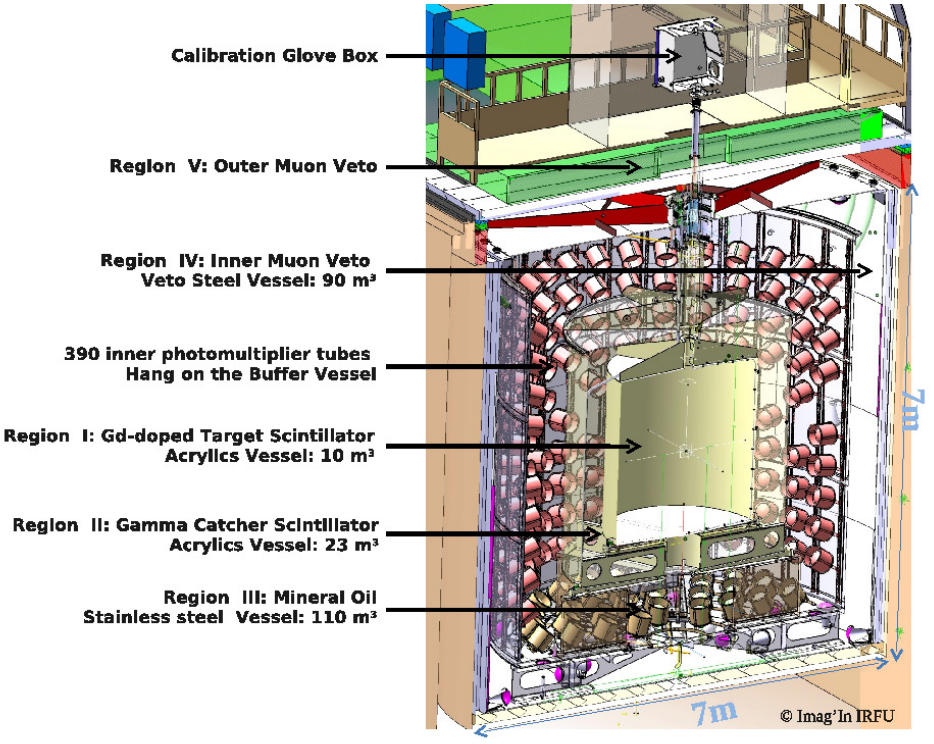


Fig. 1. – The Double Chooz detector design.

an electron. This prompt signal is followed by a delayed signal from the capture of the neutron on hydrogen or gadolinium (Gd). While the prompt signal of the positron can be considered instantaneous, the neutron capture has a time constant of about 30 μs.

3˙3. *The Far Detector*. – Figure 1 shows the composition of the Far Detector. In the center there is the *ν-Target* (Region I) consisting of 10.3 m^3 of gadolinium-loaded liquid scintillator at 1 g/l Gd-loading [7]. It is contained in a 8 mm thick cylindrical acrylic vessel and forms the fiducial volume for the search for Θ_{13}. The Target volume is surrounded by more than 22 m^3 of the so-called γ-catcher (GC) enclosed in a second acrylic vessel of 12 mm thickness (Region II). Gammas originating from the prompt and delayed event of a neutrino interaction in the Target, travel macroscopic distances while loosing their energy. The γ-catcher ensures a complete deposition of the gammas' energies and helps to reduce systematic uncertainties on the neutrino detection efficiency.

The next volume contains 114 m^3 of non-scintillating buffer liquid in a 3 mm thick stainless steel vessel (Region III). The *Buffer* volume decreases the background rates both in the prompt and delayed event originating in the ambient rock or residual radioactivity of the PMT glass. At the inner wall of the Buffer volume 390 10″ PMTs are mounted providing a coverage of about 13% [8, 9]. Finally, there is a 0.5 m thick stainless steel vessel, filled with organic liquid scintillator based on LAB (linear alkyl benzene), the so-called *Inner Veto* (Region IV). Muons and muon-induced particles entering the detector from outside produce light in the scintillator, which is then detected by 78 8″ PMTs. The

cylindrical Inner Veto vessel has a diameter of 6.5 m and a height of about 7 m, which corresponds to 90 m^3 of active muon veto. Outside the Inner Veto there are 15 cm of steel as an additional shielding to reduce background due to external gammas coming from the surrounding rock. The PMT signals are readout by 500 MHz flash-ADC hardware. The Trigger System is custom made, it forms trigger signals mainly based on the integrated charge information. Together they form a deadtime free data acquisition system [10].

On top of the cylindrical detector (Regions I-IV) a plastic scintillator strip detector serves as an additional Muon tracker, the so-called *Outer Veto* (Region V). It is superior in its vertex reconstruction capabilities compared to the Inner Veto and extends beyond the edges of it and thereby allows to veto muons, that would otherwise go undetected. The Outer Veto will help to understand and reduce the uncertainties due to muon induced backgrounds. As it has been installed slightly later than the main detector, the Outer Veto data has not been used in this analysis yet, but will be in the upcoming analysis upgrades.

4. – Calibration

Double Chooz uses the total sum of photo electrons (PE) as estimator for the deposited energy of a given event. The PEs per PMT are calculated from the charge collected in a given Inner Detector PMT, which is then multiplied by a gain factor, that has been determined from single PEs recorded with dedicated LED, that are permanently installed in the Inner Detector. The sum of PEs is calibrated with the hydrogen capture peak of the neutron source ^{252}Cf in the Target center, corresponding to 2.223 MeV. The corresponding calibration factor is about 200 PE/MeV. ^{252}Cf and γ-sources (^{137}Cs, ^{68}Ge and ^{60}Co), deployed at the Target center, have been used to study the non-linearity in energy response. A function has been determined to correct for remaining differences between data and MC, and is applied to MC on a per event basis. The same calibration sources have been deployed also at various positions in the ν-Target and in the γ-Catcher to study and correct for the variation of the detector response with position. In a similar fashion as for the non-linearity correction function, a position correction function has been determined and is also applied to the Monte Carlo data sets.

The LEDs are used to inject light into the detector on a regular basis (daily and weekly) and so this data set is used to monitor the stability of the detector response over time. The stability *vs.* time is also monitored using Spallation Neutrons capturing on H and Gd, signals induced by ambient radioactivity and Gd-captures of IBD events, see fig. 2. The stability is within 1% and in particular no degradation of the Target scintillator *vs.* time has been found.

5. – Neutrino Selection

Neutrino candidates are selected as a coincidence of a *prompt* energy deposition E_{prompt} between 0.7 and 12.2 MeV, followed by a *delayed* energy deposition $E_{delayed}$ between 6 and 12 MeV within a time difference Δt between prompt and delayed of $[2, 100]\,\mu$s. In order to avoid events from accidentally light emitting PMT bases the following cuts are applied: $Q_{max}/Q_{tot} < 0.09$ (0.06) for the prompt (delayed) energy and $\mathrm{rms}(T_{start}) < 40$ ns, where Q_{max} is the charge seen by the PMT with maximum charge, Q_{tot} is the total charge of all PMTs and $\mathrm{rms}(T_{start})$ is the standard deviation of the distribution of arrival times of pulses per PMT (and event).

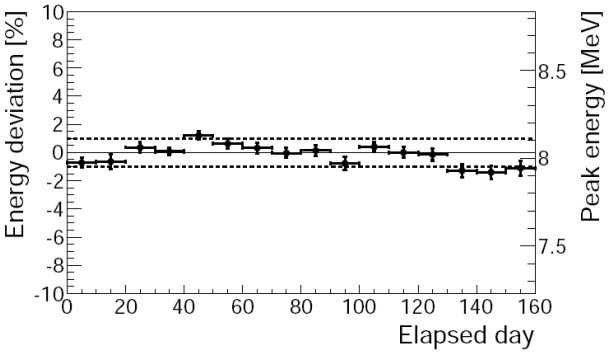


Fig. 2. – Gd peak position of IBD events *vs.* time since start of data taking (April 2011). Stability within 1% is found and in particular no degradation of the scintillators is observed [3].

To avoid neutrino-like coincidences originating from muon induced secondaries a 1 ms veto is applied after each muon interacting in the Inner Veto or Inner Detector, which results in an after muon deadtime of 4.5%. The following multiplicity cut is applied to avoid correlated background: There may not be any Trigger 100 μs before and 400 μs after the prompt energy deposition of a coincidence.

6. – Reactor prediction

The predicted number of electron anti-neutrinos interacting in the detector is proportional to the thermal power of each reactor core $P_{th}(t)$, the average energy released per fission $\langle E_f \rangle$ and the mean cross-section per fission $\langle \sigma_f \rangle$:

$$N_\nu^{pred}(E,t) = \frac{N_p \epsilon}{4\pi L^2} \cdot \frac{P_{th}(t)}{\langle E_f \rangle} \cdot \langle \sigma_f \rangle, \tag{2}$$

where N_p is the proton number in the ν-Target, ϵ is the neutrino detection efficiency and L is the distance from reactor to detector. The relative fraction of the isotopes ^{235}U, ^{239}Pu, ^{238}U, ^{241}Pu in the total fuel content enters both in $\langle E_f \rangle$ and $\langle \sigma_f \rangle$. Since the composition of the cores change with time ("burn-up"), $\langle E_f \rangle$ and $\langle \sigma_f \rangle$ are time dependent as well. Detailed simulations of the core evolution have been undertaken with two independent codes, MURE [11] and DRAGON [12] and the fission rates have been calculated. For the mean cross-section per fission improved spectra from [13] are used, while the normalisation is taken from the Bugey-4 measurement [14], with a correction to the composition of the Chooz reactors. Overall the systematic uncertainties related to the reactor amount to 1.8%.

7. – Backgrounds

The following classes of background can induce neutrino-like coincidences at the order of a few neutrino candidates per day in total.

There is *accidental background* at a rate of 0.33 ± 0.03 day^{-1}, where the prompt and delayed energy depositions are not causally linked. The prompt stems from remaining

radioactivity in the scintillator, PMTs or from the ambient rock, the delayed is a neutron-like energy deposition. The accidental background can be estimated using the off-time technique, in which the coincidence time window between prompt and delayed is shifted in time.

Three classes of *correlated background* are distinguished: ^{9}Li, *Fast Neutrons* and *Stopping Muons*. Some decay branches of ^{9}Li are β-n emitters, which can mimic IBD candidates([2]). Due to the long halflife (178 ms) of ^{9}Li it is hard to veto, given a muon rate of 46 Bq in the Inner Veto. As the ^{9}Li is being produced mainly during high-energy depositions, the ^{9}Li rate is studied using neutrino like coincidences following an energy deposition > 600 MeV. The resulting Δt_μ distribution is fitted with a constant + exponential, using the ^{9}Li halflife as time constant. Varying the muon energy cut to lower values provides an estimate of the central value and the uncertainty of the ^{9}Li rate: 2.3 ± 1.2 events/day. A shape uncertainty of 20% is coming from a MC study using variations in decay branches of ^{9}Li.

Fast Neutrons are also muon-induced background, where the prompt event is mimicked by recoil protons while the neutron is thermalizing in the γ-Catcher and Target and eventually capturing on Gd, which then forms the delayed event. Such a coincidence only is contributing to the neutrino candidates, if the muon does not pass through the Inner Veto. The rate and shape of the fast neutrons is estimated by applying the neutrino selection cuts, but expanding the prompt energy window from $[0.7, 12.2]$ MeV up to 30 MeV. Above 12 MeV one has a background only data sample, which sets the normalisation of the Fast Neutrons. The prompt energy spectrum of Fast Neutrons is taken as flat across the whole energy spectrum, including $[0.7, 12.2]$ MeV. The extrapolation of the spectral shape into the neutrino energy region has been validated using a subclass of Fast Neutron candidates, which also leave a signal in the Inner Veto and therefore allow to tag them as background even below 12 MeV. The sample of Fast Neutrons also contains a set of stopping muons, that enter the detector through the chimney region at the top of the detector. The fast neutrons (+ stopping muon component) have an estimated rate of $0.83 \pm 0.38\,\mathrm{d}^{-1}$.

The overall background rate from accidentals, fast neutrons + stopping muons and ^{9}Li adds up to $3.46 \pm 1.26\,\mathrm{d}^{-1}$. During one day in October 2011 both reactor cores were off, which allowed to perform a background-only measurement. Two neutrino-like candidates have been found, which is in good agreement with the overall background rate.

The signal to background ratio of better than 11 is illustrated in fig. 3: the selected neutrino rate contains both signal and background and still follows nicely the neutrino rate predicted from the reactor power. For the 100 days of data 4121 neutrino candidates have been selected. Taking into account for the after muon deadtime a rate of 42.6 ± 0.7 neutrinos/day is observed.

8. – Efficiencies

The Trigger Efficiency above 0.7 MeV is $100^{+0}_{-0.4}$%. The Neutron detection efficiency has been estimated with ^{252}Cf and comprises the cut efficiency of the delayed energy cut at 6 MeV (94.5% in data), the fraction of neutron captures on Gd (86.0%) and

([2]) Actually this type of background contains also a fraction of ^{8}He, which cannot be disentangled from ^{9}Li due to the low statistics and similar decay characteristics. For brevity only ^{9}Li is quoted below.

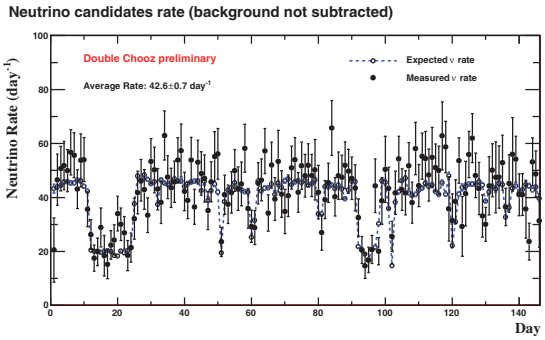


Fig. 3. – Selected and predicted neutrino rate per day *vs.* days since start of data taking. The predicted neutrino rate is calculated from the reactor data, the selected neutrino rate includes background events.

the efficiency of the ΔT_{e^+n} cut (96.5%). Uncertainties of the detection efficiency are estimated from remaining differences between data and MC and summarized in table I. A normalisation correction is applied to account for a net "Spill-In" current of 1.4%.

9. – Θ_{13} analysis

Θ_{13} is extracted using a χ^2 analysis. A "Rate-Only" (1 energy bin) and a "Rate+Shape" analysis using 17 energy bins between 0.7 and 12.2 MeV have been undertaken. In order to account for bin-to-bin correlations, four covariance matrices are used to include uncertainties from reactor, statistics, detector and background spectral shape. Both analyses give consistent results, with the "Rate+Shape" analysis being most sensitive to Θ_{13}. Our best fit result is $\sin^2(2\Theta_{13}) = 0.086 \pm 0.041$ (stat) ± 0.030 (syst) with χ^2/n.d.f. = 23.7/17. A summary of systematic uncertainties *w.r.t.* the signal is given in table I. Observed and predicted positron energy spectra for no oscillation and the best fit are shown in fig. 4.

Using a frequentist analysis, the no oscillation hypothesis is ruled out at the 94.6% CL, which can be interpreted as an indication of non-zero Θ_{13}. A combined analysis with the T2K and MINOS accelerator experimental results on θ_{13} excludes θ_{13} being equal at more than 3σ.

TABLE I. – *Systematic uncertainties on the absolute normalisation of the signal due to the detector, the reactor and backgrounds as well as the statistical uncertainty are summarized below.*

Detector	2.1%	*Reactor*	1.8%
- Energy response	1.7%	- Bugey4 measurement	1.4%
- E_{delay} containment	0.6%	- Fuel composition	0.9%
- Gd Fraction	0.6%	- Thermal power	0.5%
- ΔT_{e^+n}	0.5%	- Reference spectra	0.5%
- Spill in/out	0.4%	- Energy per fission	0.2%
- Trigger efficiency	0.4%	- IBD cross-section	0.2%
- Target H	0.3%	- Baseline	0.2%
Statistics	1.6%	*Backgrounds*	3.0%

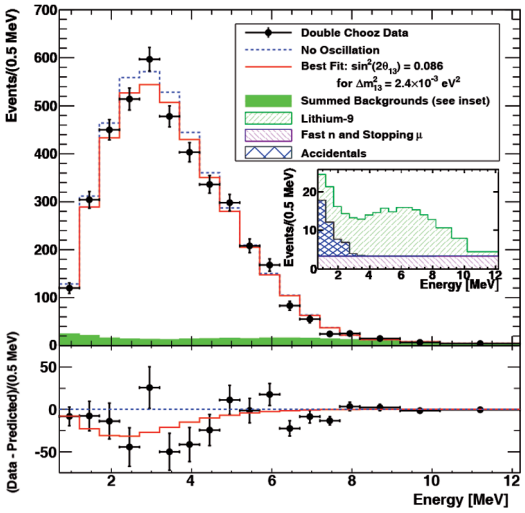


Fig. 4. – Observed (black dots) and predicted positron energy spectrum for the no-oscillation case (blue dotted line) and for the best fit value of $\sin^2 2\Theta_{13}$ (red line). The backgrounds are shown in green and the individual contributions (accidentals, ^{9}Li, Fast-n+ stopping μ) are shown in the inset. At the bottom the difference between data and the predicted no-oscillation spectrum is shown.

10. – Conclusions and outlook

A first analysis searching for Θ_{13} has been performed using data taken since April 13th, 2011. Approximately 100 days of data give a best fit of $\sin^2(2\Theta_{13}) = 0.086 \pm 0.051$ from a fit of a rate deficit and taking into account the prompt spectrum's spectral shape information. An indication of non-zero Θ_{13} is found.

Analysis improvements are already underway and the Double Chooz Near Detector will be operational soon to lead to an estimated 1σ precision of $\sin^2(2\Theta_{13}) \sim 0.02$.

REFERENCES

[1] Adamson P. *et al.*, *Phys. Rev. Lett.*, **107** (2011) 181802; arXiv:1108.0015.
[2] Abe K. *et al.*, *Phys. Rev. Lett.*, **107** (2011) 041801.
[3] Abe Y. *et al.*, *Phys. Rev. Lett.*, **108** (2012) 131801; arXiv:1112.6353.
[4] An F. P. *et al.*, *Phys. Rev. Lett.*, **108** (2012) 171803; arXiv:1203.1669.
[5] Ahn J. K. *et al.*, *Phys. Rev. Lett.*, **108** (2012) 191802; arXiv:1204.0626.
[6] Agostinelli S. *et al.*, *Nucl. Instrum. Methods A*, **506** (2003) 250.
[7] Aberle C. *et al.*, *JINST*, **7** (2012) 6008.
[8] Matsubara T. *et al.*, arXiv:1104.0786, to be published in *Nucl. Instrum. Methods A* (2012).
[9] Bauer C. *et al.*, *JINST*, **6** (2011) P06008; arXiv:1104.0758.
[10] Cabrera A., *Nucl. Instrum. Methods A*, **617** (2010) 473.
[11] *MURE, MCNP utility for reactor evolution*, 2009. `http://www.nea.fr/tools/abstract/detail/nea-1845`.
[12] Jones C. L. *et al.*, *Phys. Rev. D*, **86** (2012) 012001.
[13] Mueller Th. A. *et al.*, *Phys. Rev. C*, **83** (2011) 054615; arXiv:1101.2663.
[14] Declais Y. *et al.*, *Phys. Lett. B*, **338** (1994) 383.